JTTEE5 18:75–82
DOI: 10.1007/s11666-008-9281-2
1059-9630/$19.00 © ASM International

Corrosion Properties of Cold-Sprayed Tantalum Coatings

Heli Koivuluoto, Jonne Näkki, and Petri Vuoristo

(Submitted May 30, 2008; in revised form October 10, 2008)

Cold spraying enables the production of pure and dense metallic coatings. Denseness (impermeability) plays an important role in the corrosion resistance of coatings, and good corrosion resistance is based on the formation of a protective oxide layer in case of passivating metals and metal alloys. The aim of this study was to investigate the microstructural details, denseness, and corrosion resistance of two cold-sprayed tantalum coatings with a scanning electron microscope and corrosion tests. Polarization measurements were taken to gain information on the corrosion properties of the coatings in 3.5 wt.% NaCl and 40 wt.% H_2SO_4 solutions at room temperature and temperature of 80 °C. Standard and improved tantalum powders were tested with different spraying conditions. The cold-sprayed tantalum coating prepared from improved tantalum powder with advanced cold spray system showed excellent corrosion resistance: in microstructural analysis, it showed a uniformly dense microstructure, and, in addition, performed well in all corrosion tests.

Keywords cold spraying, corrosion properties, microstructure, tantalum

1. Introduction

Cold spraying, the latest thermal spray technique, developed in the former Soviet Union in the 1980s, is based on the use of significantly lower process temperatures with high particle velocities than those in other thermal spray techniques. A coating is formed when powder particles at high velocities (high kinetic energy) impact on the substrate, deform and adhere to substrate or other particles. In addition, good bonding between cold-sprayed powder particles requires high plastic deformation on particle impact (Ref 1-3). In cold spraying, several parameters such as particle size, particle temperature, substrate material, and the properties of the coating material affect greatly the coating formation and deposition efficiency (Ref 1, 4, 5). Because the sprayed material undergoes neither phase transformations nor melting during the spraying process (solid state process), cold spraying enables in principle the production of highly dense and pure metallic coatings (Ref 3, 6).

Chemical reactions between a material (e.g., metal, coating) and its environments can cause corrosion (Ref 7). Therefore, one important technical issue is to manufacture corrosion resistance/protective materials and coatings with specific requirements (high reliability, quality, and low costs). Corrosion resistance is necessary in several industries, in, e.g., chemical and process equipment, paper machines, and energy production systems. In many cases, protective surface coating is reportedly the best way to control corrosion, e.g., on steel products (Ref 8). Usually, the corrosion protection of many corrosion-resistant materials is based on their passivity, i.e., on the formation of a thin and protective oxide film. The passivity and protection of metals can be studied from their active-passive-transpassive behavior in anodic polarization curves (Ref 7).

Tantalum is a heavy refractory metal (atomic weight 180.948, density 16.6 g/cm^3) (Ref 9) and thus evidently suitable for cold spraying. It is also a very expensive material and therefore used only for extreme corrosion resistance. Tantalum resists corrosion effectively in acids (not HF), salts, and organic chemicals even at elevated temperatures. For example, it is highly resistant to corrosion by H_2SO_4 at a temperature of up to 200 °C. Used in chemical processing equipment and electronic devices, its corrosion resistance and inertness are based on the formation of a very thin, dense, adherent, and protective oxide layer (usually tantalum pentoxide Ta_2O_5) (Ref 10), which is a very stable compound (Ref 7). Moreover, tantalum has a low ductile-to-brittle transition temperature and a high melting temperature (2996 °C). Because ductility decreases with increasing amount of impurities (Ref 9), it should be taken into account when developing high-purity tantalum powders for cold spraying.

Tantalum coatings prepared with electrodeposition (Ref 11) and PVD (Ref 12) deposition techniques for corrosion resistance applications and with plasma spraying (Ref 13) have been reported elsewhere. Tantalum as a dense coating acts like a corrosion barrier coating on a steel substrate, providing high corrosion resistance in many environments (Ref 7). PVD (magnetron-sputtered)

Heli Koivuluoto and **Petri Vuoristo**, Department of Materials Science, Tampere University of Technology, P.O. Box 589, 33101 Tampere, Finland; and **Jonne Näkki** and **Petri Vuoristo**, Technology Centre KETEK Oy, Korpintie 8, 67100 Kokkola, Finland. Contact e-mail: heli.koivuluoto@tut.fi.

tantalum coatings have reportedly a corrosion performance equal to bulk tantalum foil (Ref 12). However, impurities and defects in the metallic coating can affect its corrosion behavior in that corrosion may arise locally from existing defects (Ref 12). Tantalum is also used as an alloying element (e.g., Ti-Ta alloys) to improve corrosion protection in sulfuric acid solutions (Ref 14). However, plasma-sprayed tantalum coatings have been shown to lack a fully dense structure in order to requirements for sealing or fusing post treatment (Ref 13).

This study sought to investigate the corrosion resistance of cold-sprayed (CS) tantalum coatings. Two different powders, standard and improved, were sprayed using different spraying parameters with two different spraying systems. The denseness of the cold-sprayed tantalum coatings was examined from scanning electron microscope (SEM) images and in corrosion tests: open-cell potential measurements and a salt spray fog test were run to assess through-porosity and polarization measurements to yield the corrosion properties of these coatings.

2. Experiments

Cold-sprayed tantalum coatings were prepared at Linde AG Linde Gas Division (Unterschleissheim, Germany). Two as-received tantalum powders from H.C. Starck GmbH (Goslar, Germany) (P1: Amperit 150.090 and P2: Amperit 151.065) were used in this study (more information on the powders in Section 3.1). The cold spray systems used were the Kinetiks 3000 and Kinetiks 4000 (Cold Gas Technology GmbH, CGT, Ampfing, Germany) high-pressure cold spray equipment with nitrogen as process gas. Kinetiks 4000 equipment is the advanced cold spray system in which can be used powder preheating, higher process temperatures and pressures, affecting particle velocities and therefore coating properties (Ref 15). In this study, CS Ta1 and CS Ta2 coatings represent two different development stages of cold-sprayed tantalum coatings. The parameters used here for cold spraying are shown in Table 1. Grit-blasted (mesh 18) carbon steel (Fe52) sheets (50 × 100 × 2 mm) were used as substrates. The reference material was a bulk tantalum sheet, supplied by Harald Pihl Ab, Sweden (ASTM B708-98 RO5200 annealed).

Microstructures of the cold-sprayed tantalum coatings were characterized using a Philips XL30 SEM. The structures were studied in unetched cross-sectional coating samples. Corrosion behavior and denseness (impermeability), i.e., the existing through-porosity of the cold-sprayed tantalum coatings, were tested with electrochemical open-cell potential measurement and a salt spray fog test. The electrochemical cell used in the open-cell potential measurements consisted of a plastic tube, of diameter 20 mm and volume 12 mL, glued on the surface of the coating specimen. A 3.5 wt.% NaCl solution was placed in the tube for 420-h measurements, taken with a Fluke 79 III true RMS multimeter. A silver/silver chloride electrode (Ag/AgCl) was used as a reference electrode. The salt spray fog test was done by following the ASTM B117 standard. Substrates were masked with epoxy paint before test in order to allow the coating surfaces only to be contact with the corroding salt spray fog. A 5 wt.% NaCl solution was used with an exposure of 240 h, a temperature of 35-40 °C, a solution pH of 6.3, and a solution accumulation of 0.04 mL/cm^2 h. The samples were characterized visually before and after exposure. Polarization measurements were taken to gain information on the corrosion resistance of the tantalum coatings. Anodic polarization tests were run adapting the standard ASTM G59. Polarization tests were run in a flat specimen cell with a rubber O-ring used as gasket. Tests were conducted in 3.5 wt.% NaCl and 40 wt.% H_2SO_4 water solutions at a room temperature (RT) of 22 °C and an elevated temperature of 80 °C. Potential was scanned from 0.6 V below the resting potential (E_0) to a potential of 3 V at a scanning rate of 2 mV/s. A saturated calomel electrode (SCE) was used for reference.

3. Results and Discussion

We investigated the microstructures and denseness of cold-sprayed tantalum coatings by SEM analysis. In addition, we evaluated the coatings' denseness and corrosion behavior with corrosion tests. Because coating denseness is important for a corrosion-resistant material such as tantalum, the first requirement is that the coating structure be of even, overall coverage.

3.1 Tantalum Powder Characteristics

We used two tantalum powders from H.C. Starck. Powder P1 was standard powder, of particle size −38 + 10 μm, as given by the producer, sprayed with a Kinetiks 3000 system (Fig. 1a). Powder P2 was improved powder, of particle size −30 + 10 μm, as given by the producer, sprayed with a Kinetiks 4000 (Fig. 1b). Figure 2 shows cumulative particle size distributions measured by laser diffraction (Sympatec Helos). Powder P2 had a finer particle size and narrower particle size distribution than powder P1. The oxygen content of P1 and P2 was 0.188 and 0.045%, respectively, measured as an average of measurements with Leco TC-436DR and Leco TC-136 chemical analyzers (Outotec Research Oy, Pori, Finland).

Table 1 Cold spray parameters and coating thicknesses

CS coating	Powder	Spray equipment	Pressure, bar	N_2 flow rate, m^3/h	Gas temperature, °C	Coating thickness, μm
CS Ta1	P1	Kinetiks 3000	32	73	530	470 (8 layers)
CS Ta2	P2	Kinetiks 4000	38	82	800	450 (3 layers)

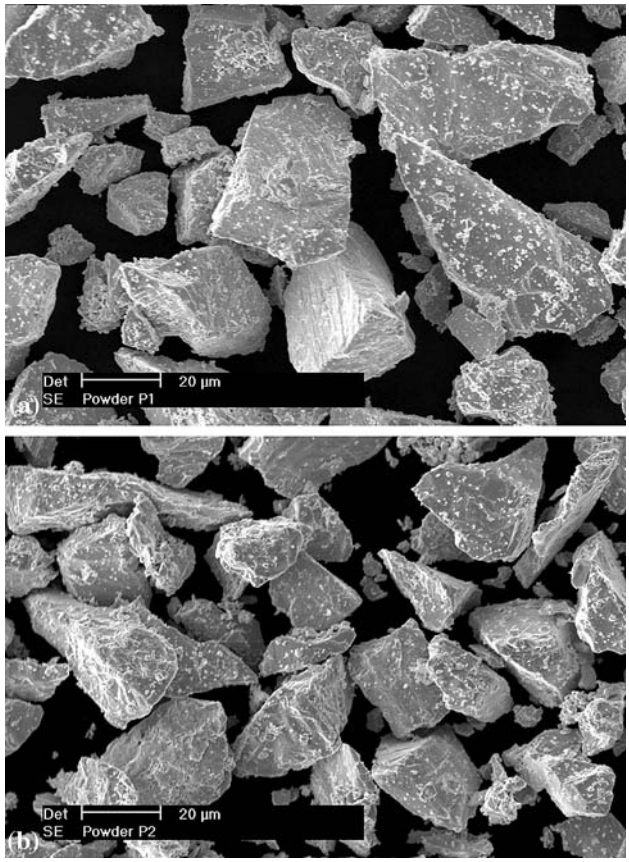

Fig. 1 Morphology of tantalum powders: (a) P1 (standard), nominal particle size −38 + 10 µm and (b) P2 (improved), nominal particle size −30 + 10 µm

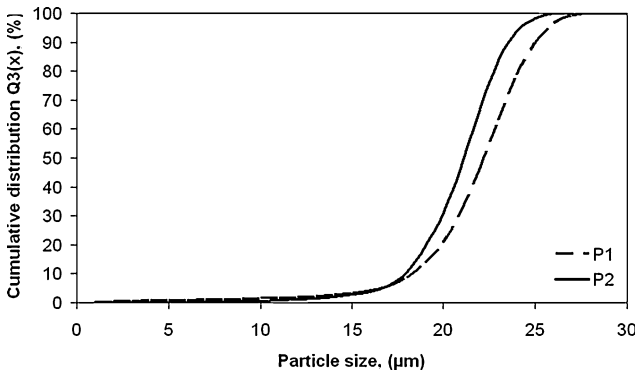

Fig. 2 Cumulative particle size distribution of powders P1 (standard) and P2 (improved) measured by laser diffraction

3.2 Microstructure of Cold-Sprayed Tantalum Coatings

Figure 3 shows a cold-sprayed tantalum coating (CS Ta1) prepared from P1 with a Kinetiks 3000 system on a grit-blasted steel substrate. Some porosity is evident in the coating structure mostly near the surface, and some defects appear in the structure (internal structure, unetched,

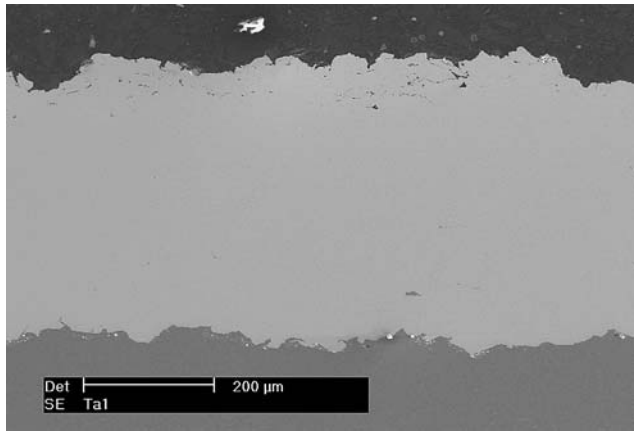

Fig. 3 Cold-sprayed tantalum coating (CS Ta1) on grit-blasted steel substrate (P1, standard)

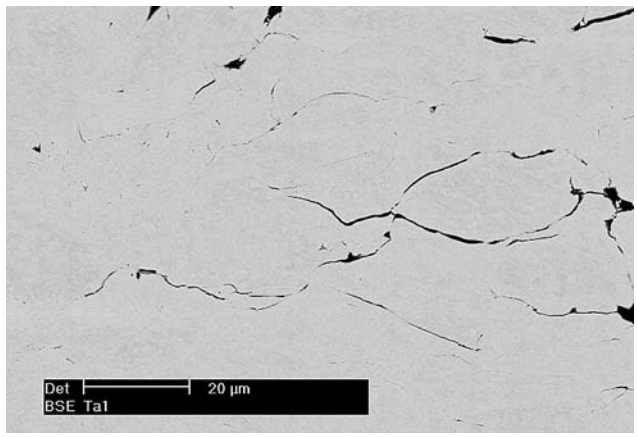

Fig. 4 Internal structure of cold-sprayed tantalum coating (CS Ta1), unetched, BSE image

shown in Fig. 4, a BSE image with high magnification). Defects, pores, and open boundaries (dark areas in Fig. 4) were observed, which are conceivable to cause poor corrosion resistance. Weak points were found in particle boundaries, reflecting locally poor adhesion between particles, and apparently oxide layers on particle surfaces not destroyed during particle impact and deformation.

Figure 5 shows the microstructure of the tantalum coating CS Ta2 prepared from improved powder P2 with a Kinetiks 4000 system on a grit-blasted steel substrate. The coating seems dense without noticeable pores. Figure 6 shows the internal structure as dense (without defects) and the interface between coating and substrate as faultless, thus testifying to a uniformly dense coating microstructure.

According to SEM analysis, CS Ta2, prepared from improved powder with advanced spraying system (Kinetiks 4000), was dense whereas CS Ta1, prepared from standard powder, contained some porosity, as evident in the SEM images (Fig. 3 and 4). These two coatings differ in their powder characteristics and spraying conditions

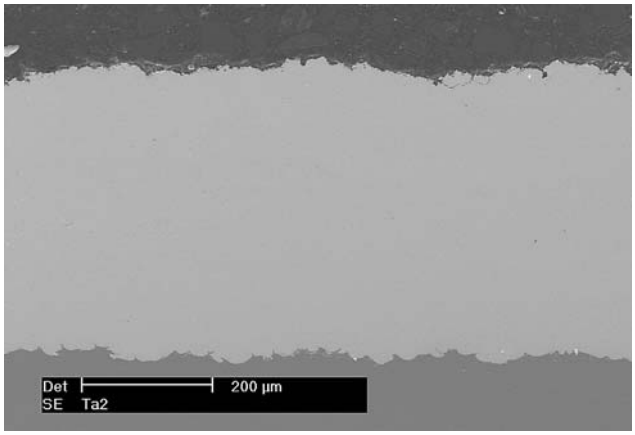

Fig. 5 Cold-sprayed tantalum coating (CS Ta2) on grit-blasted steel substrate (P2, improved)

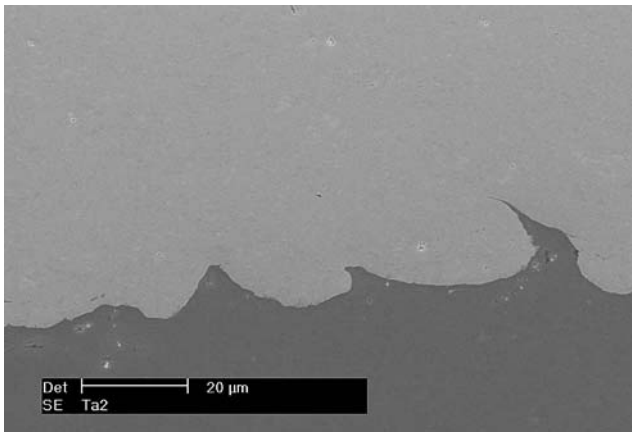

Fig. 6 Interface between cold-sprayed tantalum coating (CS Ta2) and grit-blasted steel substrate

(spraying equipment) and therefore represent tantalum coatings from two development stages. The improvement in the coating structure can be explained by an optimal combination of the powder and spray conditions. The optimal particle size for tantalum powder was $-30+10$ µm, which was slightly finer than that of the standard powder ($-38+10$ µm). Moreover, in the improved powder, the particle size distribution was slightly narrower and its purity higher than in the standard powder. Schmidt et al. (Ref 16) have reported that particle size affects on particles' impact velocities; finer particles have higher impact velocities which provide good bonds and adherence between particles and particle-substrate. On the other hand, high-purity powder particles have thinner oxide layers on the particle surfaces, promoting more tendency to get metal-metal bonding on the impact. Comparison of the microstructures of CS Ta1 (standard powder) and CS Ta2 (improved powder) reveals a significant improvement in the denseness of the cold-sprayed tantalum coating (Fig. 4 and 6).

High preheating temperatures of the process gas in the Kinetiks 4000 equipment (CGT) affect coating quality (Ref 15). First, deposition efficiency (DE) depends on gas temperature and reportedly improves at high temperature (Ref 4, 16). Second, process temperature affects the gas and particle velocity, meaning high velocity at high temperature. In addition, increased particle temperature has been reported to improve coating quality in the cold spray process (Ref 17, 18). In this study, a comparison of coating thicknesses and the number of layers sprayed revealed that DE was notably higher when the powder was sprayed with higher gas temperature (improved powder). The thickness of a single layer of CS Ta1 coating (standard, 32 bar, 540 °C) was about 60 µm and that of CS Ta2 (improved, 38 bar, 800 °C) about 150 µm. Van Steenkiste et al. (Ref 19) have also reported increased coating thickness of kinetic-sprayed tantalum coating at increased gas temperatures. On the other hand, high temperature leads to high particle velocity, which again affects coating porosity, which can increase at low particle velocity because of low kinetic energy together with less plastic deformation (Ref 19, 20). Therefore, heavy plastic deformation during particle impact (Ref 20) is crucial for efficient bonding of cold-sprayed powder particles into a dense microstructure.

3.3 Corrosion Characteristics of Cold-Sprayed Tantalum Coatings

The corrosion resistance of the cold-sprayed tantalum coatings was studied with open-cell potential measurements and a salt spray fog test to assess any existing through-porosity in the coating structure. In addition, the corrosion behavior of the coatings was compared with that of bulk tantalum in two different (3.5 wt.% NaCl and 40 wt.% H_2SO_4) testing environments (room temperature and elevated temperature) using anodic polarization measurements.

3.3.1 Open-Cell Potential Measurement. As stated before (Ref 21), open-cell potential measurement is a good method to assess any existing through-porosity (or open-porosity) in a coating structure. Because coatings are sprayed on a steel substrate, any through-porosity (allowing the test solution to penetrate the coating into the interface of coating and substrate) makes the open-cell potential of the coating approach that of the substrate. On the other hand, if the coating is dense (no existing through-porosity), the open-cell potential of the coating approaches that of the corresponding bulk material. In this study, the bulk material was a tantalum sheet and the substrate carbon steel (Fe52). Figure 7 shows the open-cell potential (reference electrode Ag/AgCl) of the tantalum bulk material (120 mV), the Fe52 bulk material (−700 mV), and CS Ta1 sprayed with standard powder (100 mV) and CS Ta2 sprayed with improved powder (−580 mV).

CS Ta2, prepared from improved powder, was structurally dense without existing through-porosity because it behaved similar like bulk tantalum during the open-cell potential measurements. In contrast, CS Ta1, prepared from standard powder, was not consistently dense because

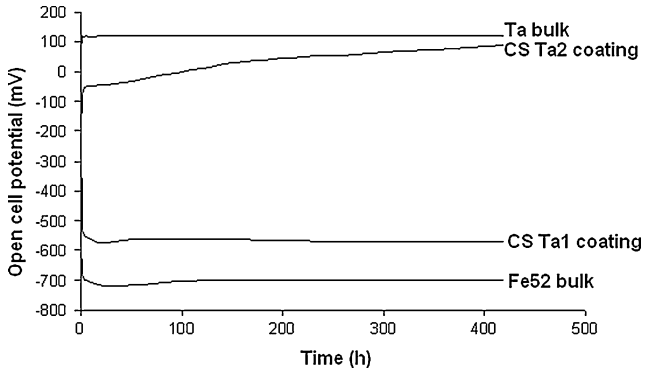

Fig. 7 Open-cell potential of tantalum (bulk material), Fe52 (substrate material), CS Ta1 (P1, standard), and CS Ta2 coating (P2, improved) as a function of exposure time with Ag/AgCl as reference electrode

its open-cell potential behavior approached that of the substrate material, suggesting existing through-porosity.

3.3.2 Salt Spray Fog Test. According to open-cell potential measurements, the CS Ta2 coating was dense; thus a salt spray fog test was run for more information about its denseness. The CS Ta1 coating was not tested because it leaked already in the open-cell potential measurements. No changes were detected on the CS Ta2 surface during exposure, indicating a uniformly dense microstructure. Figure 8 shows the surfaces of this coating taken with a digital camera before (Fig. 8a) and after a 240-h (Fig. 8b) salt spray fog test.

Open-cell potential measurement and the salt spray fog test as an auxiliary test were useful and fast methods to analyze existing through-porosity in the metallic coating structures. The salt spray fog test is a commonly used method to evaluate the quality of various coatings (Ref 22). Because tantalum is not attacked by seawater (Ref 23), these are good tests of a coating's impermeability. Because CS Ta1 showed through-porosity in corrosion tests and existing porosity in SEM studies, the key result remained the uniform denseness of the through-porosity-free CS Ta2 coatings, testifying to cold spraying's potential to produce dense, good-quality coatings. In this study, higher process temperature (CS Ta2) leads to porosity-free structure, indicating formation of tight bonds between particles and thus overall dense coating. In the cold spray process, gas preheating temperature is one of the most important spraying parameters. This study shows the effect of spraying parameters on denseness. Furthermore, strength and electrical conductivity of CS Cu coatings are reportedly improved with higher gas temperatures (Ref 16).

3.3.3 Polarization Behavior. Anodic polarization measurements were used to characterize the polarization behavior of the tantalum bulk material and the CS Ta2 and CS Ta1 coatings in two different test solutions, 3.5 wt.% NaCl and 40 wt.% H_2SO_4, at room temperature (22 °C) and at an elevated temperature (80 °C). The open-cell potential measurement and salt spray fog test already confirmed CS Ta2's overall dense structure; now its corrosion behavior and corrosion resistance were

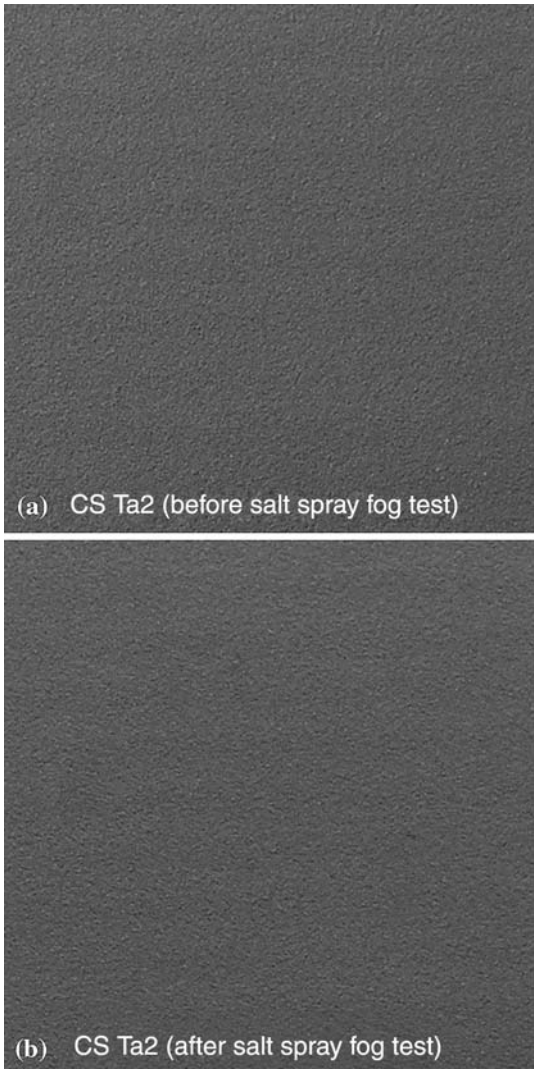

Fig. 8 Surface of CS Ta2 coating (a) before and (b) after 240-h salt spray fog test. No changes during exposure indicate dense coating structure

assessed with polarization behavior tests. The tantalum bulk material was tested for reference. The CS Ta1 coating was also tested in both solutions at room temperature for a comparison between dense structure coating (CS Ta2) and coating (CS Ta1) with through-porosity.

Figure 9 shows the anodic polarization of the tantalum bulk material and the CS Ta2 and CS Ta1 coatings in 3.5 wt.% NaCl solutions at room temperature. Tantalum gets passivated rapidly, as shown by its polarization curves in the NaCl solution, transforming linearly and quickly from active to passive with increasing potential, indicative of material stability. The CS Ta2 coating behaved like the bulk material. However, the CS Ta1 coating did not behave in a stable manner because of its through-porosity. Test solution reached with steel substrate, thus anodic polarization was a result from combination of behavior of steel substrate and CS Ta1 coating. This indicates possible instability of the passivation layer and thus provides poor

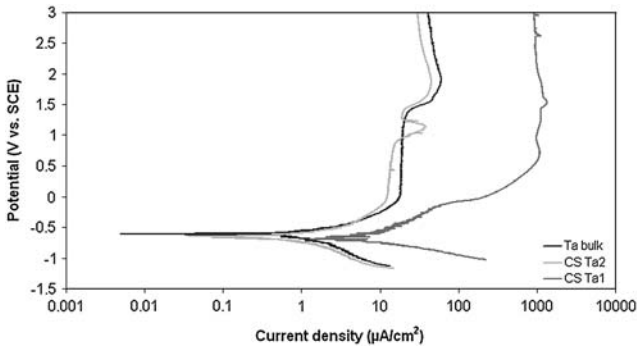

Fig. 9 Polarization behavior of tantalum bulk material, CS Ta2 (improved), and CS Ta1 (standard) coatings in 3.5 wt.% NaCl solution at 22 °C

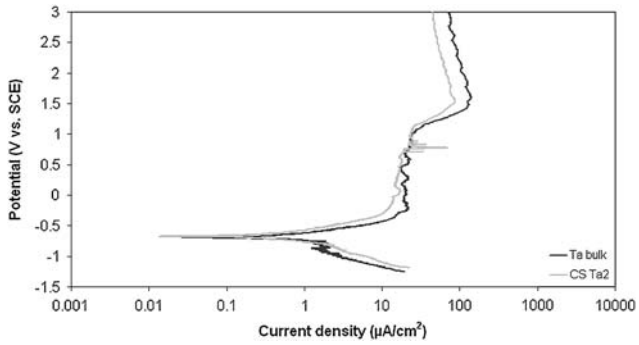

Fig. 10 Polarization behavior of tantalum bulk material and CS Ta2 (improved) coating in 3.5 wt.% NaCl solution at 80 °C

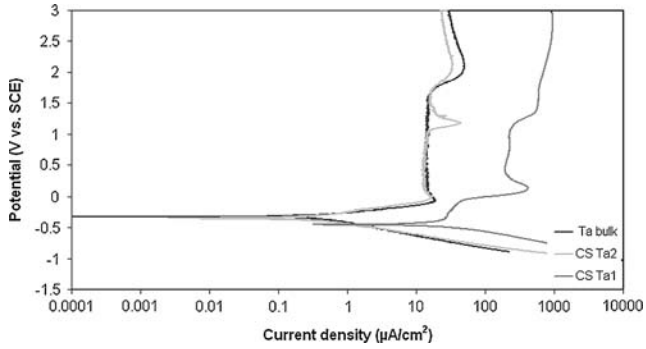

Fig. 11 Polarization behavior of tantalum bulk material, CS Ta2 (improved) and CS Ta1 (standard) coatings in 40 wt.% H_2SO_4 solution at 22 °C

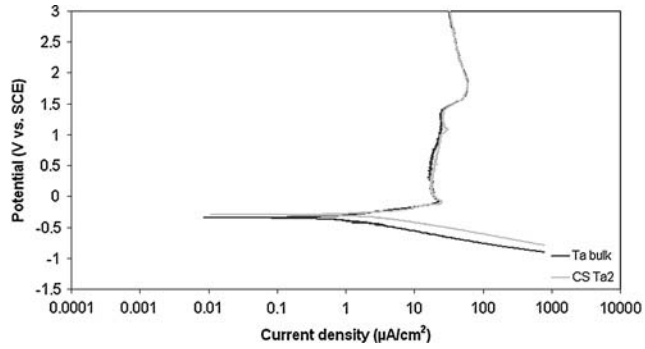

Fig. 12 Polarization behavior of tantalum bulk material, CS Ta2 (improved) coating in 40 wt.% H_2SO_4 solution at 80 °C

corrosion protection. The polarization behavior of the tantalum bulk material and the CS Ta2 coating was tested also in a 3.5 wt.% NaCl solution at an elevated 80 °C (Fig. 10). The CS Ta1 coating was not tested because of its results of existing porosity. For the results, a low current can cause some noise in the curves. The tantalum bulk material and the CS Ta2 coating showed similar polarization behavior also at the elevated temperature.

Tafel extrapolation was done from the polarization curves (Fig. 9 and 10) to determine the corrosion potential E_{corr}, passivation potential E_{pp}, corrosion current density i_{corr}, and the passivation current density i_{pp} of the tantalum bulk material and the CS Ta2 and CS Ta1 coatings (results shown in Table 2). At room temperature, CS Ta1, which lacked impermeability, showed a higher corrosion current density than the tantalum bulk and CS Ta2. The tantalum bulk and CS Ta2 got passivated rapidly, and above their passivation potential, a stable passive layer testified to a very low corrosion rate in the passive area (Ref 7).

The polarization behavior of tantalum was also investigated in an H_2SO_4 solution. Tantalum protects well against corrosion by sulfuric acid (Ref 23). Figure 11 shows the polarization curve of the tantalum bulk and CS Ta2 and CS Ta1 coatings at room temperature. As in the NaCl solution, CS Ta2 behaved here like the bulk material. However, CS Ta1 did not behave in a stable manner. At 80 °C, CS Ta2 behaved again like the bulk material, indicating capability to protect against corrosion (Fig. 12).

Table 2 Corrosion potential E_{corr}, corrosion current density i_{corr}, passivation potential E_{pp}, and passivation current density i_{pp} of tantalum bulk material, CS Ta2 and CS Ta1 coatings in 3.5 wt.% NaCl by Tafel extrapolation

Sample	Solution	T, °C	E_{corr}, V	i_{corr}, μA/cm²	E_{pp}, V	i_{pp}, μA/cm²
Ta bulk	NaCl	22	−0.66	1.1	0	16
CS Ta2	NaCl	22	−0.67	1.1	0.05	11
CS Ta1	NaCl	22	−0.68	7.1	…	…
Ta bulk	NaCl	80	−0.68	0.5	−0.25	20
CS Ta2	NaCl	80	−0.66	0.6	0.05	13

Table 3 summarizes the corrosion potential E_{corr}, passivation potential E_{pp}, corrosion current density i_{corr}, and passivation current density i_{pp} determined from the polarization curves (Fig. 11 and 12) by Tafel extrapolation. Also, here the corrosion current density of CS Ta1 exceeded that of the tantalum bulk and CS Ta2.

In summary of the polarization measurements, the CS Ta1 coating, prepared from standard powder, showed

Table 3 Corrosion potential E_{corr}, corrosion current density i_{corr}, passivation potential E_{pp} and passivation current density i_{pp} of tantalum bulk material, CS Ta2 and CS Ta1 coatings in 40 wt.% H_2SO_4 solution by Tafel extrapolation

Sample	Solution	T, °C	E_{corr}, V	i_{corr}, μA/cm^2	E_{pp}, V	i_{pp}, μA/cm^2
Ta bulk	H_2SO_4	22	−0.32	0.4	0.08	12
CS Ta2	H_2SO_4	22	−0.33	0.3	0.10	12
CS Ta1	H_2SO_4	22	−0.43	13	…	…
Ta bulk	H_2SO_4	80	−0.34	0.8	0.04	15
CS Ta2	H_2SO_4	80	−0.30	2.0	0.05	15

higher corrosion current density but no stability in its porous microstructure, whereas CS Ta2, prepared from improved powder, behaved like bulk tantalum, indicating resistance to corrosion. The latter two showed wide-ranging passivation, characteristic of stable passive behavior (Ref 24). General and pitting corrosion may occur in active areas (Ref 24). According to the polarization curves, in both NaCl and H_2SO_4 solutions, CS Ta2 passivation was first linear, then curving slightly (possibly because of pit corrosion), followed by another stretch of linear passivation at higher potential (passive layer formation). A pit may result from a failure in the passive layer (Ref 7, 23), but when pits are insignificant, reparation or repassivation and thus re-protection may occur in the protective passive layer (Ref 23). At a high potential of about 1.2 V, CS Ta2 showed unstable passivation; however, at an even higher potential the coating got repassivated. Balani et al. (Ref 6) have reported similar repassivation of cold-sprayed aluminum coatings. In fact, pitting corrosion may occur also in a transpassive area (Ref 24), and impurities may cause breaks in the passive layer (Ref 8). With some metals, passivation depends on pH and the potential (Ref 8), but the highly protective oxide layer of tantalum remains stable at all pH and potential values (Ref 7).

4. Conclusions

Cold spraying is a spraying technique capable of producing uniform dense metallic coatings by solid-state particle impacts. Because of no oxidation or melting during spraying, the coatings turn out pure and dense. In this study, we characterized two different cold-sprayed tantalum coatings (CS Ta1 and CS Ta2 from different development stages). This study reveals the importance of process parameters together with the powder type in the cold spraying. First, parameters have a very important role in the production of high-quality cold-sprayed coatings. High preheating temperature leads to high particle velocities and temperatures and further particle softening and therefore more plastic deformation occurring during impact. As is observed, process temperature affects the gas and particle velocity (Ref 4, 16). Moreover, increased particle temperature during impact reportedly improves coating quality in the cold spray process (Ref 17, 18), a fact corroborated in this study by denseness improvement. Secondly, improved tantalum powder properties were found to be the particle size and purity level. Particle size affects particle velocity and thus level of plastic deformation and coating formation. On the other hand, because tantalum is a very sensitive material to become oxidized, purity of powder particle is critical for formation of bonds between particles without micro scale defects on the boundaries. For high-pressure cold spraying, optimal tantalum powder is fused and crushed with irregular, blocky particles (−30 + 10 μm) and narrow particle size distribution. As a summary, we can notice that overall dense tantalum coating requires optimal combination of parameters and powder (particle size and purity). We suggest that gas preheating temperature is the most effective parameter, especially in the case of refractory materials with high melting temperatures. High temperature causes softening of particles and thereby tight bonds by plastic deformation.

In this study, the cold-sprayed Ta2 coating, prepared from improved powder with advanced spraying equipment (Kinetiks 4000, CGT), was microstructurally dense without noticeable pores or defects whereas the cold-sprayed Ta1 coating, prepared from standard powder (Kinetiks 3000, CGT), contained pores and weak particle boundaries. In this study, denseness was tested with corrosion tests, open-cell potential measurement, and a salt spray fog test. The results showed that CS Ta2 was impermeable with no pores in its structure. In addition, the tantalum bulk material and the coatings were tested in NaCl and H_2SO_4 solutions for their polarization behavior. CS Ta2 behaved like the tantalum bulk with rapid passivation and a high passivation range, indicative of its corrosion protection. On the other hand, CS Ta1 was not uniformly dense and thus less corrosion resistant.

High-pressure cold spraying proves its potential in the production of uniformly dense coatings. However, the powder micro- and grain structure should be studied in detail for more information on the deformation and adhesion of particles and other factors affecting dense structure formation. In future, corrosion tests will be run in more aggressive environments.

Acknowledgments

We thank Mr. Werner Krömmer, of Linde AG Gas, for the spray coatings and for his valuable advice. We also thank Dr. Karri Osara, of Outotec Research Oy, for organizing chemical analysis of the powders. This study was funded by Finnish Funding Agency for Technology and Innovation (TEKES) and a group of Finnish industrial companies.

References

1. C. Borchers, F. Gärtner, T. Stoltenhoff, H. Assadi, and H. Kreye, Microstructural and Macroscopic Properties of Cold Sprayed Copper Coatings, *J. Appl. Phys.*, 2003, **93**(12), p 10064-10070

2. R.G. Maev and V. Leshchynsky, Air Gas Dynamic Spraying of Powder Mixtures: Theory and Application, *J. Therm. Spray Technol.*, 2006, **15**(2), p 198-205
3. V.K. Champagne, *The Cold Spray Materials Deposition Process: Fundamentals and Applications*, Woodhead Publishing Limited, Cambridge, 2007, p 362
4. T. Stoltenhoff, H. Kreye, and H.J. Richter, An Analysis of the Cold Spray Process and its Coatings, *J. Therm. Spray Technol.*, 2002, **11**(4), p 542-550
5. R.C. Dykhuizen and M.F. Smith, Gas Dynamic Principles of Cold Spray, *J. Therm. Spray Technol.*, 1998, **7**(2), p 205-212
6. K. Balani, T. Laha, A. Agarwal, J. Karthikeyan, and N. Munroe, Effect of Carrier Gases on Microstructural and Electrochemical Behavior of Cold-Sprayed 1100 Aluminum Coating, *Surf. Coat. Technol.*, 2005, **195**, p 272-279
7. D.A. Jones, *Principles and Prevention of Corrosion*, 2nd ed., Prentice-Hall, Upper Saddle River, NJ, 1996, p 572
8. D.E.J. Talbot and J.D.R. Talbot, *Corrosion Science and Technology*, CRC Press LLC, 1998, p 390
9. ASM Metals Handbook Online Volume 2, *Properties and Selection: Nonferrous Alloys and Special-Purpose Materials, Pure Metals, Properties of Pure Metals, Tantalum*
10. ASM Metals Handbook Online Volume 13B, *Corrosion: Materials, Corrosion of nonferrous Alloys and Speciality Products, Corrosion of Tantalum and Tantalum Alloys*
11. S. Zein El Abedin, U. Welz-Biermann, and F. Endres, A Study on the Electrodeposition of Tantalum on NiTi Alloy in an Ionic Liquid and Corrosion Behaviour of the Coated Alloy, *Electrochem. Commun.*, 2005, **7**, p 941-946
12. S. Maeng, L. Axe, T.A. Tyson, L. Gladczuk, and M. Sosnowski, Corrosion Behaviour of Magnetron Sputtered α- and β-Ta Coatings on AISI 4340 Steel as a Function of Coating Thickness, *Corros. Sci.*, 2006, **48**, p 2154-2171
13. T. Kinos, S.L. Chen, P. Siitonen, and P. Kettunen, Densification of Plasma-Sprayed Titanium and Tantalum Coatings, *J. Therm. Spray Technol.*, 1996, **5**(4), p 439-444
14. K.A. de Souza and A. Robin, Influence of Concentration and Temperature on the Corrosion Behavior of Titanium, Titanium-20 and 40% Tantalum Alloys and Tantalum in Sulfuric Acid Solutions, *Mater. Chem. Phys.*, 2007, **103**, p 351-360
15. H. Hoell and P. Richter, KINETIKS® 4000 – New Perspective with Cold Spraying, *Thermal Spray 2008: Thermal Spray Crossing Borders*, DVS, June 2-4, 2008 (Maastricht, The Netherlands), p 2
16. T. Schmidt, F. Gärtner, and H. Kreye, New Developments in Cold Spray Based on Higher Gas- and Particle Temperatures, *J. Therm. Spray Technol.*, 2006, **15**(4), p 488-494
17. P. Richter and H. Höll, Latest Technology for Commercially Available Cold Spray Systems, *Thermal Spray 2006: Building on 100 Years of Success*, B.R. Marple, M.M. Hyland, Y.-C. Lau, R.S. Lima, and J. Voyer, Eds., May 15-18 (Seattle, Washington, USA), ASM International, p 3
18. H. Kreye, T. Schmidt, F. Gärtner, and T. Stoltenhoff, The Cold Spray Process and Its Optimization, *Thermal Spray 2006: Building on 100 Years of Success*, B.R. Marple, M.M. Hyland, Y.-C. Lau, R.S. Lima, and J. Voyer, Eds., May 15-18 (Seattle, Washington, USA), ASM International, p 5
19. T. Van Steenkiste and D.W. Gorkiewicz, Analysis of Tantalum Coatings Produced by the Kinetic Spray Process, *J. Therm. Spray Technol.*, 2004, **13**(2), p 265-273
20. T.H. Van Steenkiste, J.R. Smith, and R.E. Teets, Aluminum Coatings Via Kinetic Spray with Relatively Large Powder Particles, *Surf. Coat. Technol.*, 2002, **154**, p 237-252
21. H. Koivuluoto, J. Lagerbom, and P. Vuoristo, Microstructural Studies of Cold Sprayed Copper, Nickel, and Copper-30% Nickel Coatings, *J. Therm. Spray Technol.*, 2007, **16**(4), p 488-497
22. Standard Test Method of Salt Spray (Fog) Testing, B117-90, *Annual Book of ASTM Standards*, ASTM, p 19-25
23. P.A. Schweitzer, Ed., *Corrosion Engineering Handbook*, Marcel Dekker, 1996, p 736
24. W.S. Tait, *An Introduction to Electrochemical Corrosion Testing for Practicing Engineers and Scientists*, Pair O Docs Publications, Racine, WI, 1994, p 138